Dynamics of the glassforming liquid di2ethylhexyl phthalate (DOP) as studied by light scattering and neutron scattering

G. Floudas, J. S. Higgins, and G. Fytas

Citation: The Journal of Chemical Physics **96**, 7672 (1992); doi: 10.1063/1.462368
View online: http://dx.doi.org/10.1063/1.462368
View Table of Contents: http://scitation.aip.org/content/aip/journal/jcp/96/10?ver=pdfcov
Published by the AIP Publishing

Dynamics of the glass-forming liquid di-2-ethylhexyl phthalate (DOP) as studied by light scattering and neutron scattering

G. Floudas[a),b)] and J. S. Higgins
Imperial College, Department of Chemical Engineering, London SW7 2BY, England

G. Fytas
Research Center of Crete, P.O. Box 1527, 711 10 Heraklion Crete, Greece

(Received 23 September 1991; accepted 3 February 1992)

Dynamic light scattering (depolarized Rayleigh and polarized Rayleigh–Brillouin) and quasielastic neutron scattering are employed to study the dynamics of the glass-forming liquid di-2-ethylhexyl phthalate (DOP) ($T_g = 184$ K). The depolarized Rayleigh scattering measurements were made in the temperature range from 303 to 433 K, the polarized Rayleigh–Brillouin measurements in the range from 263 to 433 K, and the quasielastic neutron-scattering measurements in the range from 37 to 312 K and in the Q range from 0.33 to 1.84 Å^{-1}. The orientation times for DOP, obtained from a single Lorentzian fit to the experimental depolarized spectra at high T, are in good agreement with recent dielectric data for the primary (α) relaxation. However, at lower T, the viscosity increases more strongly than the orientation times and the Stokes–Einstein–Debye equation which can adequately describe the dynamics in the high-T range is insufficient at temperatures close to T_g. The relaxation time obtained from the Rayleigh–Brillouin experiment is about 1 order of magnitude faster than the orientation times. In the neutron-scattering experiment we find a strong decrease of the elastic intensity and a corresponding increase of the quasielastic intensity around T_g. The data analysis with respect to the dynamics (from a two Lorentzian fit) revealed the existence of three processes affecting the high-frequency range: (i) a "fast" ($\tau_2 \sim 10$ ps) Q-independent motion with weak T dependence ($E_2 = 1.54$ kcal/mol), (ii) a "slow" Q-dependent motion, and (iii) a flat background increasing with T and Q. The fast process is discussed in terms of a very localized motion of the phenyl group (β relaxation) and, as such, as a precursor of the the primary (α) relaxation. The relaxation time of this process (τ_2) was found to compare nicely with the time τ_{max} from the Rayleigh–Brillouin (RB) experiment suggesting that the latter is caused by fast localized motions. The slow process is discussed in terms of the jump-diffusion model. The activation energy associated with the jump-diffusion times is 6.1 kcal/mol and it is associated with large-scale diffusional motion of the DOP molecule. The relaxation times obtained from this process are compared with the relaxation times obtained from the depolarized and dielectric techniques for the primary relaxation. Finally, the background can be identified with fast local motions and/or low-frequency excitations relaxing outside the energy window of our experiment.

I. INTRODUCTION

Density fluctuations are of central interest in recent experimental[1] and theoretical[2] investigations of the glass transition. These fluctuations are present in any system: small molecules, macromolecules, and combinations of small molecules with macromolecules. When the dynamics of small molecules and macromolecules are compared with respect to density fluctuations at temperatures near the glass transition temperature (T_g) they exhibit very similar features: The density correlation function is described by a stretched exponential with a degree of stretching depending on the complexity and cooperativity of the system; the relaxation times for the density fluctuations slow down considerably as we approach T_g and the temperature (T) dependence of the relaxation times is described by the Vogel–Fulcher–Tammann (VFT) equation over a broad T range.[3] However, Rouse–Zimm normal modes, reptation, and entanglement effects are slow motions of polymeric nature. In this respect the study of density fluctuations in simple glass-forming liquids is less complicated. The dynamics of density fluctuations can be measured by dynamic light scattering (DLS) and quasielastic neutron scattering (QNS) over a broad frequency and temperature range.

Traditional techniques such as mechanical relaxation (MR),[4] photon correlation spectroscopy (PCS),[5] etc. are usually employed to study the dynamics of small molecules and macromolecules at temperatures around T_g. However, the temperature range of interest has recently been shifted to higher temperatures. This was a result of the molecular "clusters" observed in a number of systems well above T_g,[1] and of recent mode coupling theory (MCT) which predicts a dynamic instability at a temperature around $1.2T_g$.[2] In this temperature range, interesting phenomena seem to occur. The Stokes–Einstein–Debye (SED) equation which describes the dynamics of supercooled liquids at high tempera-

[a)] Author to whom correspondence should be addressed.
[b)] Present address: Max-Planck-Institut für Polymerforschung, Postfach 3148, D-6500 Mainz, Germany.

 0021-9606/92/107672-11$06.00

tures fails in a number of systems as we approach T_g from high temperatures.[6,7] It may also not be accidental that in this high-T range more than one relaxation process is detected.[8] The primary (α) relaxation is observed from T_g to $T_g + 150$ K with different techniques. The strong T dependence associated with this process is a result of large-scale segmental relaxation. Secondary relaxations (β,γ) are studied from $T < T_g$ up to $T_g + 150$ K. These are localized processes with weak T dependence which are known to play an important role in polymer dynamics, not only as a precursor of the α relaxation but also as an intrinsic feature of molecular glasses.[9]

The purpose of the present study is to investigate the dynamics of density fluctuations in a simple supercooled liquid in the high-frequency/temperature range. For this reason we employ DLS (depolarized Rayleigh and polarized Rayleigh–Brillouin) in the T range 263 to 433 K and QNS in the T range from 37 to 312 K. With DLS and QNS we study the dynamics of di-2-ethylhexyl phthalate (DOP) in the frequency range from GHz to THz. Furthermore, we compare our results with recent dielectric relaxation[10] (DR) measurements made on the same liquid over a broad frequency/temperature range. This latter comparison between relaxation times obtained from different techniques has been successfully attempted in a number of systems before mainly with the use of DR, MR, and DLS.[11,12] However, comparison with relaxation times obtained from QNS experiments is not straightforward since the relaxation process studied by QNS can have an additional Q dependence as well as the normal T dependence. It is, to our knowledge, the first time that a sequence of Q-dependent relaxation times obtained from QNS is compared with the relaxation times obtained from other techniques. This was made possible with the inclusion of a third axis to the usual two-dimensional Arrhenius plot displaying the additional Q dependence of the relaxation times. We suggest that from such a plot processes related to the glass transition can easily be identified.

II. EXPERIMENTAL SECTION

Di-2-ethylhexyl phthalate (DOP) ($T_g = 184$ K, $\rho = 0.981$ g/cm^3, $n_{20^\circ} = 1.485$) was purchased from Aldrich and was used without further purification. In the light-scattering experiment DOP was filtered through a 0.22 μm Millipore filter directly into the dust-free scattering cell. In both, the light-scattering and the neutron-scattering experiments, attention was paid to avoid crystallization.

The depolarized Rayleigh spectra (DRS) $I_{VH}(\omega)$ were obtained at a scattering angle (θ) of 90°. The excitation source was an argon-ion single-mode laser (Spectra Physics 2020), operating at $\lambda = 488$ nm with a stabilized power of 100 mW. Details on the apparatus can be found elsewhere.[13] Two free spectral ranges (FSR) were used: 7.62 and 16.96 GHz with a finesse of better than 60. The temperature range covered was from 30 to 160 °C. Typical $I_{VH}(\omega)$ spectra are shown in Fig. 1 at three temperatures. Polarized Rayleigh–Brillouin spectra $I_{VV}(\omega)$ were recorded in the temperature range − 10–160 °C at a scattering angle of 90°. The FSR used was 25.3 GHz and the finesse was in the range 55–75.

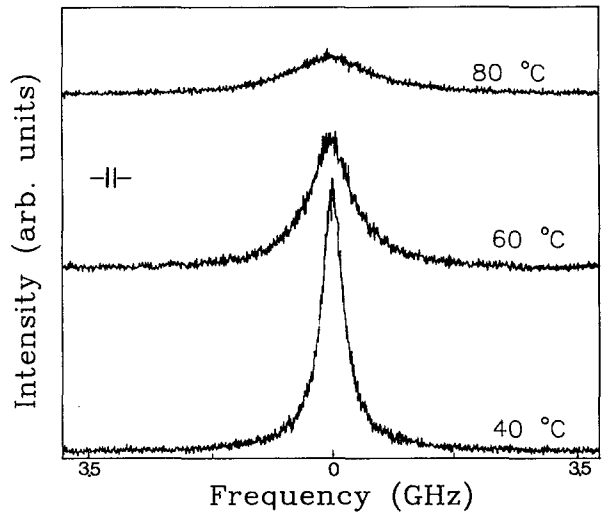

FIG. 1. Depolarized Rayleigh spectra $I_{VH}(\omega)$ of DOP at three temperatures as indicated. The symbol -||- denotes the instrument FWHH.

Typical $I_{VV}(\omega)$ spectra are shown in Fig. 2 at three temperatures.

The neutron-scattering experiment was carried out on the IRIS backscattering spectrometer at the ISIS pulsed neutron source at the Rutherford Appleton Laboratory (RAL). Neutron spectra were recorded simultaneously with 51 pyrolitic graphite and 51 mica detectors distributed over 2π in the scattering plane. The pyrolitic graphite 002 and the mica 006 reflections were used in the present study with an energy resolution of 15 and 11 μeV, respectively, over a Q range from 0.33 to 1.84 Å^{-1}. The energy range covered was from − 0.4 to 0.4 meV. The DOP sample was contained in a flat Al container and the sample thickness was set to 0.2 mm—in order to minimize multiple scattering—resulting in a trans-

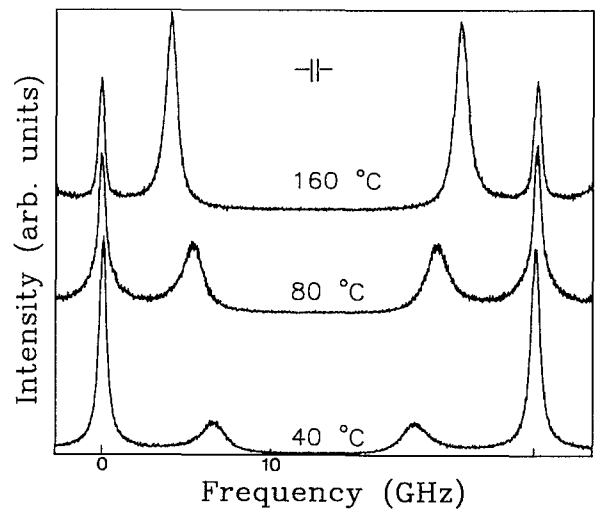

FIG. 2. Polarized Rayleigh–Brillouin $I_{VV}(\omega)$ spectra of DOP at three temperatures as indicated. The symbol -||- denotes the instrument FWHH.

mission of about 89%. The Al container was mounted in a liquid-helium cryostat at 45° to the incident neutron beam. Before the experiment the sample was heated up to 310 K for about 30 min and then cooled down to the set temperature. While cooling at approximately 0.8 K/min down to the lowest temperature (37 K) we monitored the neutron intensity scattered at zero energy transfer. In this way, the temperature dependence of the elastic scattering intensity, $S(Q,\omega\simeq 0)$, was determined and is depicted in Fig. 3. Then, we performed long-time measurements at selected temperatures: 37, 260, 285, and 312 K. The temperature stability was better than 2 K during these runs. Spectra at 260, 285, and 312 K show a characteristic quasielastic broadening plus a background in addition to the elastic peak shown at the lowest temperature (37 K). Typical spectra at different temperatures for $Q = 1.62$ Å^{-1} are shown in Fig. 4. In Fig. 5, the Q variation is shown at 312 K.

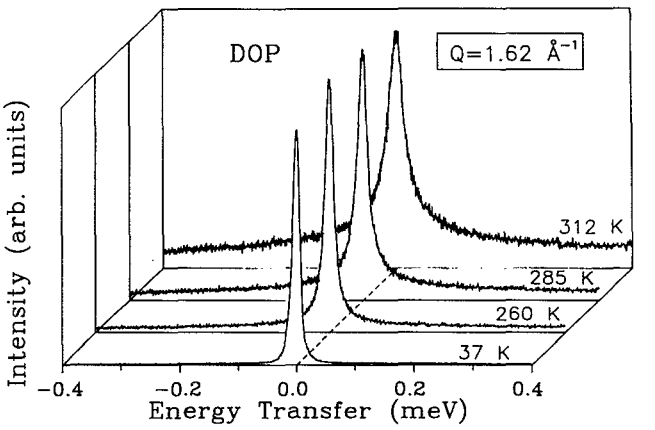

FIG. 4. Quasielastic neutron-scattering spectra of DOP at different temperatures at $Q = 1.62$ Å^{-1}. The lowest measured temperature ($T = 37$ K) corresponds to the resolution function used in the convolution procedure.

III. DATA ANALYSIS

Analysis of the $I_{VH}(\omega)$ spectra (Fig. 1) consisted of fitting about 800 points per peak with a single Lorentzian plus a base line,

$$I_{VH}(\omega) = \frac{1}{\pi} I \frac{\Gamma}{\Gamma^2 + \omega^2} + B, \tag{1}$$

where I and Γ are the integrated intensity and the half-width at half-height (HWHH) and B is the background. The $I_{VH}(\omega)$ spectra (Fig. 1) did not show the central dip, which is observed under certain conditions.[14] For a liquid composed of optically anisotropic molecules these conditions are met when the value of the quantity $Q^2\eta/\rho$, where Q is the scattering wave vector, η the viscosity, and ρ the density, is comparable to the overall HWHH Γ. In practice, the central dip is observed when $Q^2\eta/\rho\Gamma$ is in the range 0.1–0.7 and the value of the coupling R—characterizing the coupling between the shear waves of the fluid with molecular orientation—is sufficiently large (0.1 or greater).[15] For DOP the ratio $Q^2\eta/\rho\Gamma$ is outside this range at all interferometric temperatures, thus explaining the absence of the central dip from the experimental spectra.

The total integrated depolarized intensity is given by[16]

$$I_{VH} = Af(n)\rho^*\gamma_{eff}^2, \tag{2}$$

where A is a constant, $f(n)$ is the product of the local-field correction and the geometrical factor $1/n^2$, ρ^* is the number density of the anisotropic scatterers, and γ_{eff}^2 is the effective optical anisotropy. Using the integrated intensity and $\rho = 0.981$ g/cm^3 and $n = 1.485$ for the density and refractive index, respectively, we obtain an effective optical anisotropy of 32 Å^6 for DOP. It is the relatively high optical anisotropy of DOP which makes the detection of a signal from this liquid possible in the DRS experiment. The temperature dependence of the DRS spectra taken at a FSR of 7.62 GHz is

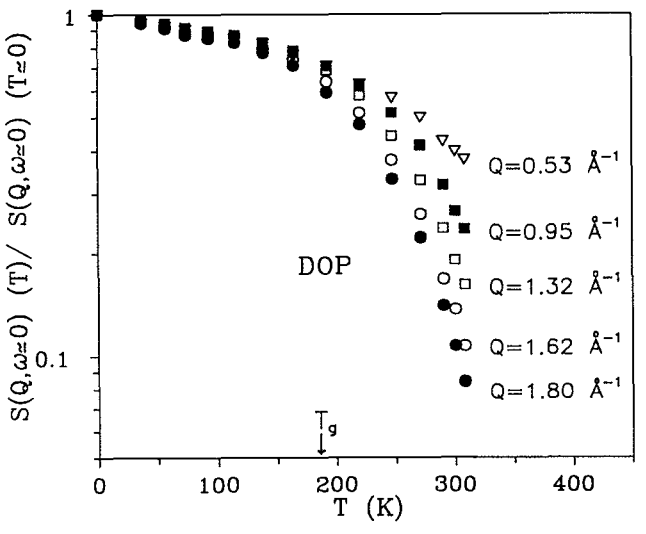

FIG. 3. Temperature dependence of the incoherent dynamic structure factor $S(Q,\omega\simeq 0)$ of DOP normalized to its value at $T = 0$ K, plotted for selected Q values. Data points are averaged within an interval of ± 0.1 Å^{-1} about the indicated Q values. At $T < T_g$ a strong Q-dependent decrease of the elastic intensity is observed as a result of a motion (see text).

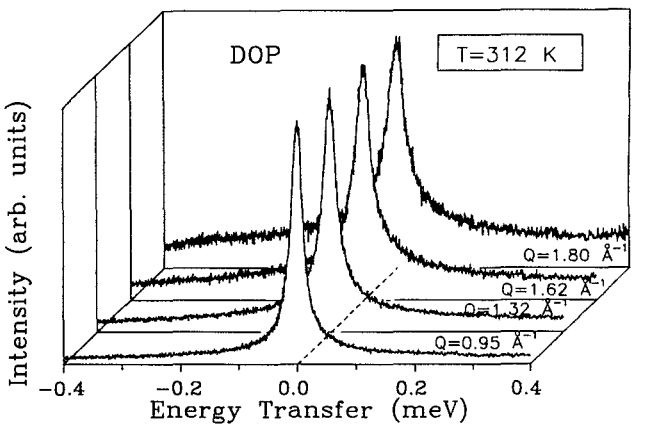

FIG. 5. Quasielastic neutron-scattering spectra of DOP at different Q values at $T = 312$ K.

shown in Fig. 1. The HWHH Γ exhibits strong temperature dependence and for this reason all spectra above 80 °C were measured with a higher FSR (16.96 GHz). The true HWHH (Γ) was obtained after convolution with the instrument line shape. The collective orientation relaxation time τ_{or} was then computed from

$$\tau_{ori} = \frac{1}{2\pi\Gamma}. \tag{3}$$

The $I_{VV}(\omega)$ spectra (Fig. 2) consist of three central components and two shifted Brillouin peaks. The unshifted line corresponds to the resolution function, the "mountain" peak and the I_{VH} contribution. I_{VH} contributes to I_{VV} because at $\theta = 90°$ and for uncorrelated density and polarizability fluctuations[16] $I_{VV} = I_{iso} + (4/3)I_{VH}$, where I_{iso} is due to density fluctuations. In the polarized RB spectroscopy we are mainly interested in the dispersion of the Brillouin linewidth Γ_B and shift f_B. The former is related to sound attenuation ($\alpha = \pi 2\Gamma_B/u$), whereas the latter to sound velocity ($u = f_B/Q$). The fitting procedure to the Brillouin lines involves a Lorentzian function plus the overlap from the neighboring interferometric orders. After subtraction of the instrument linewidth—due to the high finesse—the Brillouin shift f_B and linewidth $2\Gamma_B$ are obtained. The Landau–Placzek (R_{LP}) intensity ratio, defined as the ratio of the central peak (after subtraction of the I_{VH} contribution) to the total Brillouin intensity, was also calculated and will be discussed in the next section.

Neutron scattering from DOP is dominated by the incoherent scattering of hydrogen atoms, because DOP contains C, O, and H atoms and the incoherent scattering of hydrogen is much higher than the incoherent and coherent cross sections of carbon and oxygen.[17] Thus, to a good approximation, quasielastic neutron scattering measures the incoherent dynamic structure factor,

$$S_{inc}(Q,\omega) \sim \int \exp(-i\omega t) I_S(Q,t)\,dt \sim \int \exp(-i\omega t)\langle \exp\{-iQ\cdot[R_i(0) - R_i(t)]\}\rangle dt, \tag{4}$$

where $I_S(Q,t)$ is the intermediate scattering function and $R_i(0)$, $R_i(t)$ are the positions of the i th nucleus at times 0 and t. $S_{inc}(Q,\omega)$ gives information on both the dynamics and the geometry of the single-particle dynamics. After the initial neutron counts were corrected for detector, monitor efficiency, and for background effects, the time-of-flight (TOF) cross section $\vartheta^2\sigma/\vartheta\Omega\vartheta\tau$ was plotted vs τ, where τ is the neutron TOF scattered into a solid angle $\vartheta\Omega$. The observed TOF spectra were converted to a differential scattering cross section $\vartheta^2\sigma/\vartheta\Omega\vartheta E$ and the incoherent scattering law $S_{inc}(Q,\omega)$ was calculated from

$$S_{inc}(Q,\omega) = \frac{k_i}{k_s}\frac{1}{(\langle b^2\rangle - \langle b\rangle^2)}\frac{\partial^2\sigma}{\partial\Omega\partial E}, \tag{5}$$

where k_i and k_s are the incident and scattered wave vectors, respectively, and b is the scattering length for hydrogen atoms.

Two kinds of experiments were made with the incoherent quasielastic neutron-scattering technique. In the first experiment, only neutrons with zero energy transfer (or with energy transfer smaller than the IRIS resolution function) are counted giving $S(Q,\omega\approx 0)$. This quantity can be equated to the long-time limit of the intermediate scattering function $I_S(Q,t)$ [Eq. (4)]. $S(Q,\omega\approx 0)$ was measured for different Q values in the range 0.33–1.84 Å^{-1} and in the temperature range from 37 to 312 K. Values normalized relative to the extrapolated intensity at 0 K are shown in Fig. 3 for different Q values.

At low temperatures, below the glass transition temperatures, $S(Q,\omega\approx 0)_T/S(Q,\omega\approx 0)_{T=0}$ can be described by the Debye model for harmonic solids, i.e.,

$$S(Q,\omega\approx 0)\sim e^{-\langle r^2\rangle Q^2}, \quad \langle r^2\rangle \sim T. \tag{6}$$

Thus, $\ln S(Q,\omega\approx 0)_T/S(Q,\omega\approx 0)_{T=0} \sim -T$, according to this model, and our data for DOP agree with this prediction for $T \ll T_g$. A pertinent feature of Fig. 3 is the extra decrease of the elastic intensity at temperatures below the calorimetric T_g. This extra decrease in the elastic intensity is strongly Q dependent at higher temperatures as seen in Fig. 3. The fact that the elastic intensity decreases beyond the values expected from Eq. (6) is an indication of motion which starts already below T_g. To verify this finding we have made a second experiment where we measured $S(Q,\omega)$ at three temperatures between 265 and 312 K. A low-temperature measurement was also made (37 K) which served as the resolution function. The spectra in Fig. 4 show a quasielastic broadening at 265, 285, and 312 K along with an increasing background. The Q dependence shown in Fig. 5 at 312 K exhibits similar behavior: a Q-dependent quasielastic broadening and an increasing background. The trends in the intensities with T and Q are discussed later in detail.

In the literature different approaches have been reported to fit the quasielastic neutron-scattering spectra at $T > T_g$.[18–20] In view of the DR measurements on DOP over a broad frequency/temperature range[10]—where the distribution of relaxation times narrows to a single relaxation time at high T—we have fitted the QNS spectra using a single Lorentzian plus a base line. However, such a fit produced strong deviations from the experimental data. The second simplest function—which gives a good fit to all experimental data—is a sum of two Lorentzians plus a base line,

$$S_{inc}(Q,\omega) = \frac{1}{\pi}I_1(Q)\frac{\Gamma_1(Q)}{\Gamma_1^2(Q)+\omega^2} + \frac{1}{\pi}I_2(Q)\frac{\Gamma_2(Q)}{\Gamma_2^2(Q)+\omega^2} + B. \tag{7}$$

In Eq. (7), I_1 and I_2 are the integrated intensities of the narrower and broader Lorentzians, respectively, and Γ_1 and Γ_2 the corresponding HWHH. The Q dependence of the two components is depicted in Fig. 6 at 312 K. It is worth noticing that (i) the narrower Lorentzian broadens considerably

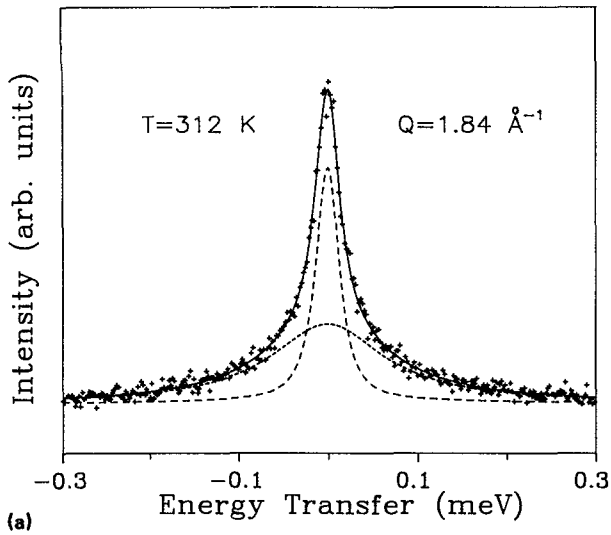

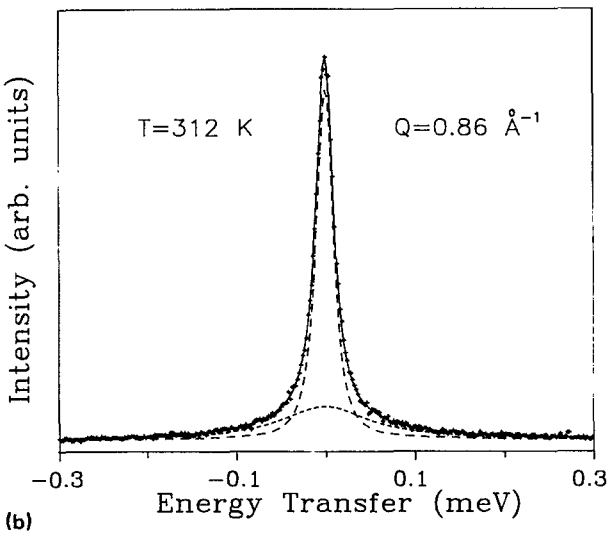

FIG. 6. (a) Quasielastic neutron-scattering spectrum of DOP at $T = 312$ K and $Q = 1.84$ Å^{-1} showing the narrow and broad Lorentzian components (dashed lines). The solid line represents the result of the fit of Eq. (7) to the experimental points (+). (b) Quasielastic neutron-scattering spectrum of DOP at $T = 312$ K and $Q = 0.86$ Å^{-1}.

with increasing Q, whereas the linewidth Γ_2 of the broader component is nearly Q independent, and (ii) the relative intensity of the narrower component I_1^* ($= I_1/I_1 + I_2$) increases with decreasing Q at the expense of the relative intensity of the broader component I_2^*. These features of the experimental data will be discussed in detail in the next section.

IV. RESULTS AND DISCUSSION

A. Light scattering

The dependence of the collective orientation relaxation time τ_{or} obtained from Eq. (3) on the macroscopic viscosity is usually described by the modified SED equation,[21]

$$\tau_{\rm ori} = \frac{g_2}{j_2}\left(\frac{V_h}{k_B}\frac{\eta_S}{T}\right) + \tau_\infty , \tag{8}$$

where V_h is the effective hydrodynamic volume of the reorienting molecule, g_2 and j_2 are the static and dynamic pair orientation correlation parameters, respectively, and τ_∞ is the nonzero intercept in the limit $\eta/T \to 0$. Using the temperature dependence of the measured shear viscosity in the temperature range $223 < T < 372$ K,[22]

$$\log \eta_S = -3.92 + \frac{537}{T - 152.2}, \tag{9}$$

and the orientation times in the temperature range $320 < T < 372$ K, we obtain

$$\tau_{\rm ori} = (77 \pm 5)\times 10^{-12}\ \text{s} + \frac{\eta}{T}(11 \pm 1)\times 10^{-9}\frac{sK}{cP}. \tag{10}$$

From Eq. (10) we obtain a hydrodynamic volume at high temperatures of 150 ± 20 Å^3. The effective hydrodynamic volume for DOP, obtained at high temperatures, is similar to the one reported earlier for the glass former aroclor (A1248).[7] This is consistent with the similar orientational dynamics of the two solvents at high temperatures as obtained by DRS.

The temperature dependence of f_B and $2\Gamma_B$, obtained from the $I_{VV}(\omega)$, shown in Fig. 7, resemble that usually found in both polymeric[23] and nonpolymeric viscoelastic liquids.[24] The Brillouin shift decreases continously with increasing temperature, whereas the Brillouin linewidth increases, reaches a maximum at about 20 °C and then decreases at low but nonzero values. The effects have been shown to be due to structural relaxation in the GHz frequency range. The characteristic time due to structural relaxation is obtained from the frequency $f_{\max}$ at which $2\Gamma_B$ attains its maximum value (Fig. 7): $\tau_{\max} = 1/2\pi f_{\max} \approx 2.2\times 10^{-11}$ s. Little is known about the molecular mechanism responsible for the Brillouin maximum at hypersonic frequencies. Our

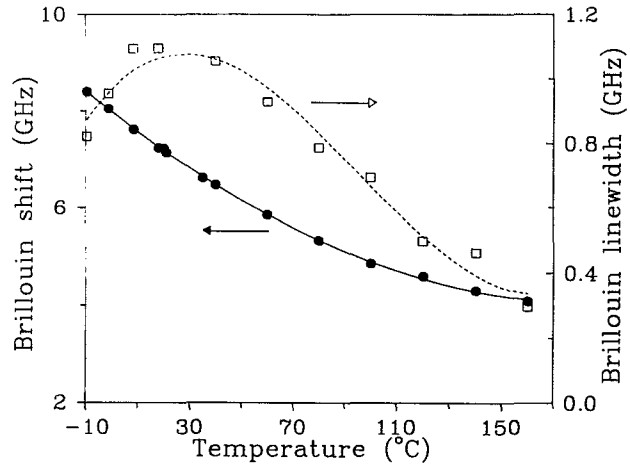

FIG. 7. Brillouin shift (●) and Brillouin linewidth (□) for DOP as a function of temperature.

present neutron-scattering data (see next section) provide valuable information with respect to the fast structural relaxation observed in the Rayleigh–Brillouin experiment.

The temperature dependence of the Landau–Placzek (LP) ratio for DOP is shown in Fig. 8. This ratio is given by[25]

$$R_{\mathrm{LP}} \sim \gamma \frac{M(\omega)}{M_0} - 1 = \gamma \left[\frac{u(\omega)}{u_0}\right]^2 - 1, \qquad (11)$$

where $M(\omega)$ $[=\rho u^2(\omega)]$ is the real part of the adiabatic longitudinal modulus at frequency ω, M_0 $(=\rho u_0^2)$ is the longitudinal modulus at zero frequency, and γ is the ratio of the specific heats at constant pressure and volume. For a nonrelaxing liquid, Eq. (11) reduces to $\gamma - 1$. As shown in Fig. 8, in the high-temperature range, the R_{LP} depends only slightly on temperature, with values close to the ones expected for nonrelaxing simple liquids, i.e., $R_{\mathrm{LP}} = 0.2$. However, at lower temperatures R_{LP} increases strongly. The strong increase of R_{LP} at low T is only partially due to the existence of structural relaxation [Eq. (11)]. Assuming a T independent γ ($\simeq 1.2$) and the measured sound velocities we can calculate the R_{LP} from Eq. (11). The calculated values are also shown in Fig. 8. Evidently, there exists a discrepancy between the measured and the calculated values. High R_{LP} values were also reported recently for other glass-forming liquids.[26] To explain these effects, it was postulated that in the supercooled liquid, above T_g, "prefreezing" phenomena occur which give rise to the "excess" scattering ("clusters"). The formation of these "clusters" depends on the thermal history of the sample. It has also been reported that for the glass-former *o*-terphenyl (OTP) it was possible to prepare samples with and without "clusters" in a reproducible way.[1] The values of the R_{LP} ratio for the OTP sample with clusters were much higher than for those without.

The formation of clusters in supercooled liquids well above T_g,[1] and/or the dynamic instability predicted by recent MCT (Ref. 2) at $T \simeq 1.2T_g$ could be related with the breakdown of the SED equation [Eq. (8)] observed in a number of systems within a narrow temperature range above T_g.[6–8] In these systems the solvent orientation time τ_{or} does not scale with η/T except at the highest temperatures, where Eq. (8) is valid. In the viscous regime, the viscosity increases more strongly than the orientation time and this was demonstrated by a discontinuity in the plot of τ/η_S vs T_g/T at a temperature $T_c \simeq 1.2T_g$. In a recent study of the glass-forming liquid aroclor (A1248),[7] the observed breakdown of the SED equation was discussed in terms of the formation of molecular clusters at temperatures well above T_g which gave rise to an increase in the polarized light-scattering intensity and consequently to the very high R_{LP} values. Since both DOP and A1248 display higher LP ratios than those predicted by Eq. (11) and for the latter the breakdown was experimentally observed it is tempting to plot the τ/η values of DOP as a function of T^{-1}. This is demonstrated in Fig. 9 where we plot $\tau - \tau_\infty/\eta$ vs T_g/T, for orientation times obtained from the present DRS and DR experiments. It is worth mentioning that data points for τ/η in Fig. 9 are calculated from the measured orientation times and by interpolating the existing viscosity data[22] [Eq. (9)]. It is evident from Fig. 9 that the breakdown of the SED equation occurs at $T_g/T \sim 0.7$–0.8. At high T_g/T values the slope $\partial(\tau/\eta)/\partial(1/T)$ is negative as was observed in other supercooled liquids.[6] In a similar plot for A1248,[7] the breakdown of the SED equation occurred at even lower temperatures ($T_g/T \sim 0.8$–0.85) and it was more pronounced than in DOP and more clearly observed because of the existence of viscosity data close to T_g.

B. Neutron scattering

The full width at half height (FWHH) $2\Gamma_1$ and $2\Gamma_2$ of the narrower and broader Lorentzians, obtained from Eq.

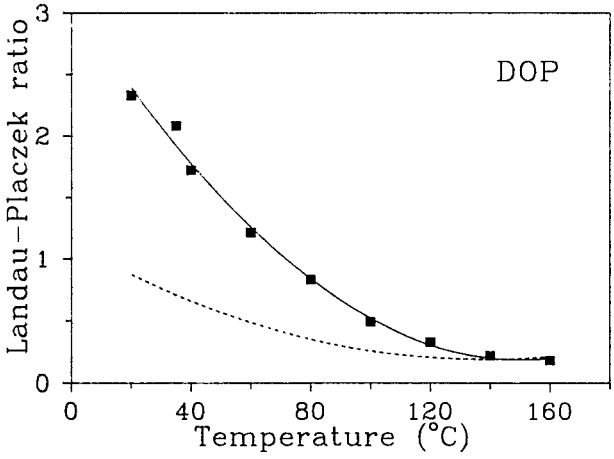

FIG. 8. Landau–Placzek (R_{LP}) intensity ratio of DOP as a function of temperature. The solid line is a guide to the experimental points. The dashed line is the calculated $R_{\mathrm{LP}}(T)$ using Eq. (11).

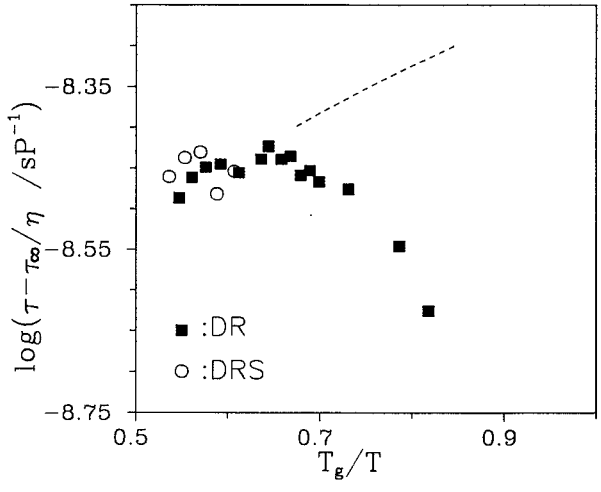

FIG. 9. $\tau - \tau_\infty/\eta$ as a function of reduced inverse temperature. Orientation times are obtained from DRS (○) and DR (■). The dashed line is a plot of Eq. (10) at high T and demonstrates the breakdown of this equation as we approach T_g.

(7), are plotted in Figs. 10(a) and 10(b) as a function of Q^2 and Q, respectively. A pertinent feature of Fig. 10 is that the two processes are separated by about 1 order of magnitude in the time (or frequency) scale and that they display different Q and T dependence. Γ_2, of the broader component, is independent of Q and shows a very a weak T dependence ($E_2 = 1.54$ kcal/mol), suggesting that this component is due to a very localized motion. On the other hand, Γ_1 of the narrower component is Q^2 dependent at small Q and shows a weaker Q dependence at higher Q values. The latter process displays a strong T dependence in contrast to the former process. Clearly, in the double Lorentzian representation, the two distinct relaxation processes observed in the neutron-scattering experiment [Figs. 10(a) and 10(b)] cannot belong to a single mode of motion.

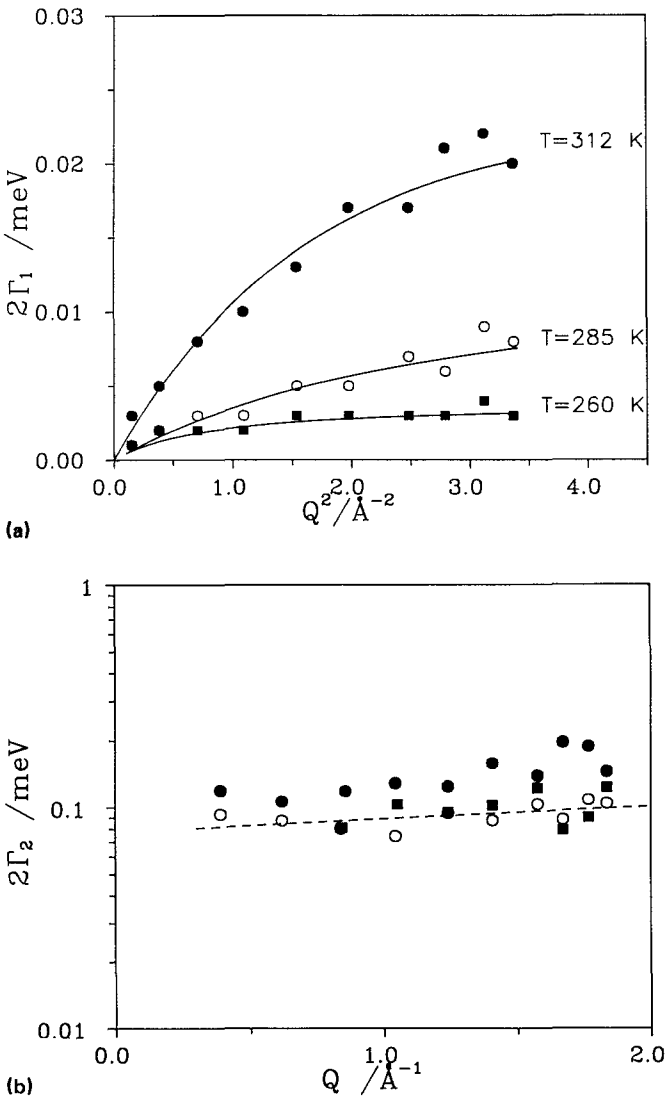

FIG. 10. (a) Q^2 dependence of the full width at half maximum (FWHM) of the narrow quasielastic component $2\Gamma_1$, at three temperatures as indicated. The solid lines are from the fit to the jump-diffusion model. (b) Q dependence of the FWHH of the broad neutron-scattering quasielastic component $2\Gamma_2$, at three temperatures: (●) $T = 312$ K; (○) $T = 285$ K; (■) $T = 260$ K.

The peculiar behavior of the slower motion can be discussed in terms of the jump-diffusion model.[27] This model has been proposed by Singwi and Sjölander to explain the diffusive motion of hydrogen-bonded water molecules.[28] In this model there are two relevant times: the rest time τ_1^*, during which the proton undergoes oscillatory motions about a center of equilibrium, building up a thermal cloud and the jump time τ_2, during which the particle diffuses from one configuration to another. The main hypothesis of the model is that the protons remain in a given configuration for a much longer time than they diffuse (i.e., $\tau_1^* \gg \tau_2$). The dynamic structure factor is then given by

$$S(Q,\omega) = e^{-\langle r^2\rangle Q^2} \frac{1}{\pi} \frac{\Gamma_1}{\Gamma_1^2 + \omega^2}, \tag{12}$$

$$\Gamma_1(Q) \sim \frac{1}{\tau_1^*}\left(1 - \frac{e^{-\langle r^2\rangle Q^2}}{1 + Q^2 D \tau_1^*}\right). \tag{13}$$

The shape of the quasielastic peak due to jump diffusion is Lorentzian with HWHH given by Eq. (13). In the limit of small Q values, Eq. (13) is reduced to DQ^2. Clearly, at small Q (or at long distances) the details of the elementary jump process cannot be observed and the quasielastic broadening is given by Fick's law. On the contrary, at large Q values the quasielastic broadening tends asymptotically to τ_1^{*-1}, and the linewidth strongly deviates from Fick's law.

Our experimental results for Γ_1 [Fig. 10(a)] can be described by the jump-diffusion model. Applying Eq. (13) to the experimental data we have evaluated the best values for D and τ_1^* at the three temperatures studied. The root-mean-square amplitude $\langle r^2\rangle^{1/2}$ evaluated from Eq. (6) and the parameters $\langle l^2\rangle^{1/2}$ (calculated from $D \simeq \langle l^2\rangle/6\tau_1^*$) and τ_1^* from the jump-diffusion model along with the times for the Q-independent process (τ_2) are summarized in Table I. $\langle l^2\rangle^{1/2}$ exhibits a weak temperature dependence which is opposite to that of $\langle r^2\rangle^{1/2}$. This is not surprising since at higher temperatures the mean-square jump distance can be reduced due to the increasing dimensions of the developed thermal cloud. A temperature-dependent $\langle l^2\rangle^{1/2}$ has been observed in the study of hydrogen-bonded water,[28] and in a recent study of bulk polybutadiene (PB).[29] In the former study the T dependence has been interpreted in terms of the random network model of water. We should point out, however, that the determination of D—and consequently of $\langle l^2\rangle$

TABLE I. Parameters of the jump-diffusion model.

T (K)	$\langle r^2\rangle$ (Å^2)	$\langle l^2\rangle^{0.5}$ (Å)	τ_1^* (ps)[a]	τ_2 (ps)[b]
260	0.38	1.9	371.8	15.3
285	0.53	1.3	122.6	13.8
312	0.73	1.4	52.9	9.3

[a] Activation energy of τ_1^*: $E_1 = 6.1$ kcal/mol.
[b] Activation energy of τ_2: $E_2 = 1.54$ kcal/mol.

—from the fit to Eq. (13) is subject to some error mainly because D is determined by $\Gamma_1(Q)$ at small Q where the deconvoluted linewidth is equal to or smaller than the instrument resolution. On the other hand, values of τ_1^* are obtained from $\Gamma_1(Q)$ at high Q—from the fit to Eq. (13)—where the error is small.

The activation energy associated with the jump-diffusion times τ_1^* can be obtained from an Arrhenius fit to the experimental times τ_1^*,

$$\log \tau_1^* = \log \tau_{10}^* + \frac{E_1}{2.3RT}. \tag{14}$$

The fit to Eq. (14) yields the apparent activation energy $E_1 = 6.1$ kcal/mol with $\log \tau_{10}^* = -14.53$ (in s). Evidently, the relaxation time τ_1^* exhibits strong temperature dependence in contrast to that of τ_2 which has an activation energy of $E_2 = 1.54$ kcal/mol. The former time (τ_1^*) is associated with large-scale motion of the DOP molecules as a whole and this time is comparable with the relaxation times obtained from other techniques for the primary relaxation (see next section). From this point of view, the broadening of the narrow component (Γ_1) is due to long-scale diffusive motions which can be described by the jump-diffusion model. These motions are associated with the primary (α) relaxation and monitor the glass transition in the neutron-scattering frequency range.

Apart from the dynamics of the "fast" and "slow" NS processes we are also interested in the integrated intensities I_1 and I_2 extracted from the fit to Eq. (7). As already mentioned in the data analysis with respect to Fig. 6, the relative intensity of the narrower component I_1^* ($= I_1/I_1 + I_2$) decreases with increasing Q and the intensity lost reappears into the broader component I_2^*. This experimental finding deserves more attention. It demonstrates that although the dynamics of the two processes are well separated the relative intensities (I_1^* and I_2^*) are correlated over the Q and T range studied. In Fig. 11, the Q dependence of the relative intensities I_1^* and I_2^* is shown at three temperatures. The $I_1^*(Q)$ dependence of the slow NS process can also be viewed as an apparent elastic incoherent structure factor (EISF),[17] since at the high temperatures of the present study there is no fixed center of mass. As seen in Fig. 11, both increasing T and increasing Q produces a similar increase in I_2^*. Evidently, the fast process becomes more intense at high T and Q through the mechanism $I_1 \rightarrow I_2$. On the other hand, the increase of I_1^* at low Q and the concomitant decrease of I_2^* can explain the fact that the fast process affects the NS experiment more than the light scattering. It is probably because of the small intensity I_2^* as $Q \rightarrow 0$ that this process was not detected in the DRS experiment. An alternative interpretation to this could be that the fast NS process may not change significantly the molecular polarizability. Therefore, it is the unique advantage of the NS experiment that components with Q-dependent intensity can be studied in the high-frequency range.

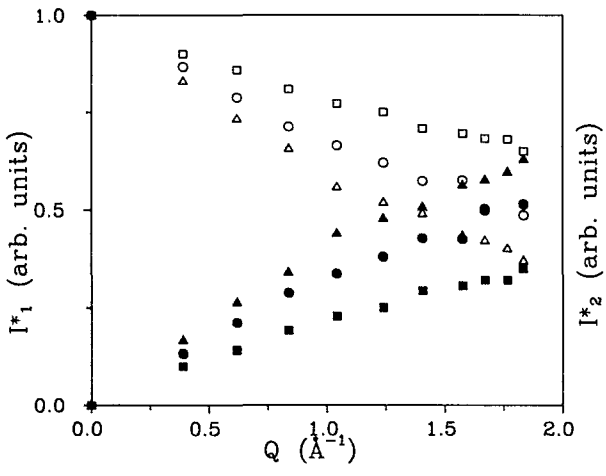

FIG. 11. Q dependence of the relative quasielastic neutron-scattering intensities I_1^* ($= I_1 + I_2$) (open symbols) and I_2^* ($= I_2/I_1 + I_2$) (solid symbols) for different temperatures: (Δ,▲) $T = 312$ K; (○,●) $T = 285$ K; (□,■) $T = 260$ K.

We are now left with the task of identifying the molecular processes behind the broad quasielastic component and the T- and Q-dependent background (Figs. 4 and 5). The fast process associated with the broad quasielastic broadening exhibits a weak T dependence ($E_2 = 1.54$ kcal/mol) and is independent of Q over the Q range from 0.33 to 1.84 Å^{-1}. The weak T dependence and more important the Q independence implies that it is a very localized, nondiffusive type of motion. It could be that this process is related to a libration or a pseudorotational motion of the phenyl group. On the other hand, it cannot be due to reorientation of the whole molecule because the reorientational times obtained from the DRS experiment are much longer (in ns time scale). Recently, fast processes displaying weak T dependence have been reported for the glass-forming liquids orthoterphenyl (OTP) and bis-phenol-C-dimethylether[30] (BCDE) by DRS and DR techniques, respectively. The fast process observed in the DRS spectra of OTP had a nearly constant relaxation time (~3 ps) over 180 K. Furthermore, the $I_{VH}(\omega)$ intensity of this process was temperature dependent, being higher at high T, in agreement with the present fast component. The dielectrically active β process observed in BCDE had an activation energy of ~1.6 kcal/mol. This secondary relaxation was discussed in terms of a π-phenyl flip in view of ^{2}H–NMR solid echo measurements. Alternatively, the fast process observed in our NS experiment and in the above-mentioned DRS and DR studies can be identified as the β relaxation due to fast density fluctuations suggested by the mode coupling theory.[2]

The significant background observed in the NS experiment is due to even faster localized motion with T- and Q-dependent intensity. Ester methyl group rotations in selectively deuterated poly(methyl methacrylate) (PMMA) have been studied extensively from room temperature down to 60 K.[31,32] The observed motion was predominantly a threefold symmetric rotation about the O–CH_3 bond with an activation energy of ~1.7 kcal/mol at high T. Assuming similar activation parameters for the methyl groups in DOP to those for the ester methyl group in PMMA, we find a quasielastic broadening of 0.84 meV (FWHH) and 0.64 meV at 300 and 265 K, respectively. Similarly, the methyl

group rotation studied in poly(methylphenyl siloxane) (PMPS) (Ref. 33) at 300 K contributes to a quasielastic broadening of 0.82 meV. However, quasielastic broadening of the order of 0.8 meV appears nearly as a flat background within the energy window of our experiment. Moreover, the increase with T of the background could reflect increase in I_2^*, which may imply an increasing number of methyl groups participating in this local rotational motion.[32] This is reflected in the decrease of the EISF with increasing T at a given Q value (Fig. 11). Furthermore, an increasing background with Q at a given T could reflect the usual Q dependence of the EISF for this motion. The low-temperature excitations in the low-energy inelastic range 1–4 meV (Ref. 34) observed in a number of systems provide an alternative explanation for the background. The observed increase in the intensity of this peak with increasing temperature is consistent with the T-dependent background. Therefore, these excitations relaxing outside the energy range of our spectrometer could explain qualitatively this feature of our experimental spectra.

C. Interelations between light-scattering and neutron-scattering times

In Fig. 12(a), we plot the relaxation times obtained from DRS, RB, DR, and the fast Q-independent NS times. A pertinent feature of Fig. 12(a) is the good agreement between the DRS and DR times for the primary (α) relaxation and between the RB $\tau_{\max}$ with the fast NS times. The solvent dynamics are probed by DRS and DR through the optical anisotropy and dipole moment, respectively. Both techniques are sensitive to motions of orientational character since these motions influence the quantity on which optical anisotropy and dipole moment depend: the macroscopic polarizability. However, the ratio of the orientation times $\tau(l=1)/\tau(l=2)$ [$= 1/l(l+1)$, where $\tau(l)$ is the orientation time for the lth-order spherical harmonic] obtained from DR ($l=1$) and DRS ($l=2$), is 1 and not 1/3, in agreement with experimental results[35] and recent models of rotational relaxation.[36] It is interesting to note that this agreement holds at $T \gg T_g$ for DOP.

The τ values as obtained by DRS and DR, conform to the VFT expression,

$$\log \tau = \log \tau^* + \frac{B}{T - T_0}. \tag{15}$$

A least-squares fit of Eq. (15) to the DRS and DR data of Fig. 12(a) yields $\tau^* = 0.9 \pm 0.1$ ps, $B = 496 \pm 10$ K, and $T_0 = 150.9 \pm 1$ K. The corresponding viscosity data yield $B_\eta = 537 \pm 10$ K and $T_0 = 152.2 \pm 1$ K [Eq. (9)]. The stronger temperature dependence of the viscosity data than the $\tau(T)$ is reflected in the value of B_η being about 8% higher than B. This is the main reason for the breakdown of the SED equation discussed earlier.

The relaxation time $\tau_{\max}$, obtained from the linewidth maximum in the RB experiment, is different from the orientational times τ_{or} and from the DR times by at least 1 order of magnitude.[1,22(c),33,37] The relaxation time $\tau_{\max}$ reflects a *faster* motion than that probed by DR and DRS. Evidently, reorientation of the axis that involves the greatest change of polarizability, which gives rise to DRS and DR, is too slow to follow the sound propagation in the GHz frequency range. In the present study we find good agreement between the fast NS times τ_2 with the RB $\tau_{\max}$. We believe that this is not a coincidence, but underlines a common mechanism in the GHz frequency range. In the recent incoherent neutron-scattering PMPS study[33] it was found that the β relaxation associated with the π flip of the phenyl ring occurred in the same frequency as the RB $f_{\max}$, although this finding was not discussed. We suggest that the fast NS process observed in the ps time scale is a kind of β relaxation for the DOP molecule which affects mainly the NS experiment because of intensity reasons (the arguments were discussed in terms of Fig. 11). The additional information obtained from our NS results with respect to the Q and T dependence suggests that hypersonic attenuation in the GHz frequency range is

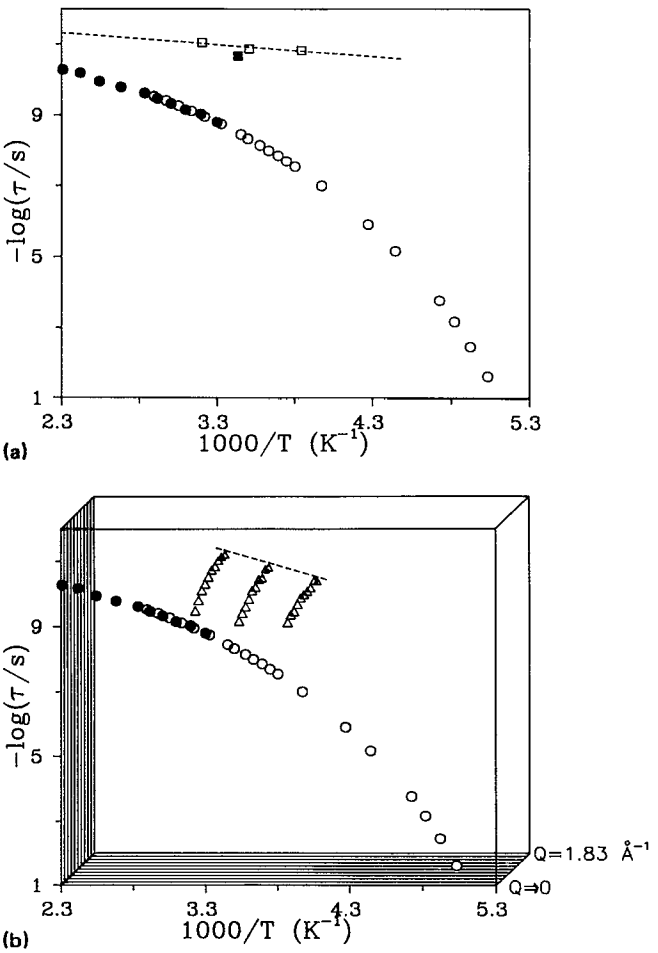

FIG. 12. (a) Arrhenius plot of the relaxation times obtained by depolarized Rayleigh scattering (●), dielectric relaxation (○), Rayleigh–Brillouin scattering (■), and fast neutron-scattering process (□). (b) 3 D Arrhenius representation of the relaxation times of the primary (α) relaxation of DOP, obtained from depolarized Rayleigh scattering (DRS) (●), dielectric relaxation (DR) (○), and from the slow neutron-scattering process (Δ) plotted for different Q values in the range from 0.4 to 1.83 Å^{-1}. DRS and DR times are located on the front plane ($Q \to 0$).

caused by fast localized motions. The molecular mechanism behind the RB and fast NS process could then be related to libration motion of the phenyl group. Similarly, in a recent study of propylene carbonate[20] a good agreement between the RB τ_{max} and the NS process—obtained from a single Lorentzian fit—was observed, with the NS and RB data displaying an Arrhenius T dependence.

Comparison of Q-dependent NS relaxation times with times obtained from DRS, DR, PCS, and NMR experiments provides an enormous challenge. Frequently, in the literature,[20,38,39] a Q value has been chosen at which the NS relaxation times happen to coincide with the relaxation times obtained from other techniques for the primary relaxation of polymeric and nonpolymeric glasses. In Fig. 12(b), we attempt to resolve this ambiguity by introducing a third axis to the usual two-dimensional Arrhenius plot to account for any Q-dependent processes. In Fig. 12(b), the Q dependence of the slow NS process due to jump diffusion is plotted and compared with the Q-independent DRS and DR times for DOP. Evidently, the NS relaxation times $\tau_1(Q)$ $[=1/2\pi\Gamma_1(Q)]$, are influenced by the *same process* (α relaxation) *at different* Q.[40] We thus justify our earlier claim that the broadening of the narrow NS component (Γ_1) is due to long-range motions associated with the glass transition. However, because of the limited instrument resolution we cannot follow the dynamics of the primary relaxation to longer times.

V. CONCLUDING REMARKS

Depolarized and polarized light scattering and neutron scattering were employed to study the dynamics of the glass-forming liquid DOP over a broad temperature range. The orientation times obtained from a single Lorentzian fit to the experimental $I_{VH}(\omega)$ spectra are in good agreement with recent dielectric measurements. DRS and DR probe the primary (α) relaxation over a broad temperature and frequency range and the orientation times can be well described by the VFT equation.[41] The SED equation which adequately describes the dynamics in the high-temperature range fails as we approach T_g from high temperatures.[42] This finding is consistent with the notion of clustering and with recent mode coupling theory which predicts a dynamic instability above T_g.

The neutron-scattering experiment revealed the existence of additional processes operating at higher frequencies. The slow NS process with its peculiar Q dependence was discussed in terms of the jump-diffusion model. This process with an apparent activation energy of about 6 kcal/mol is associated with large-scale diffusional motion of the DOP molecule as a whole (α relaxation). The Q dependent NS relaxation times were compared with the DRS and DR times for the primary relaxation with the construction of a "three-dimensional" (3D) Arrhenius plot where the third axis displays the additional Q dependence. The NS times $\tau_1(Q)$ for the slow process were influenced by the primary relaxation at different Q values. The fast Q-independent NS process with activation energy of 1.5 kcal/mol was discussed in terms of a very localized motion of the phenyl group (β relaxation). This process affects primarily the NS experiment because of the intensity of the scattering process. Furthermore, this fast process was found to operate in the same frequency range as the characteristic frequency of the Rayleigh–Brillouin experiment, suggesting that dispersion and sound attenuation in the latter experiment is caused by fast localized motions.

ACKNOWLEDGMENTS

The authors are grateful to the Rutherford Appleton Laboratory for use of the experimental facilities at ISIS and particularly to Dr. W. S. Howells for computational assistance, and to Dr. C. Carlile and Mr. M. Adams for assistance during the experiment. G.F. thanks Professor E. W. Fischer, Professor H. Sillescu, and Dr. G. Meier for helpful discussions. Valuable comments on the manuscript by Professor A. Patkowski are highly appreciated. We are indebted to the Science and Engineering Research Council (SERC) and Imperial Chemical Industries (ICI) for a research fellowship (G.F.).

[1] See, for example, E. W. Fischer, G. Meier, T. Rabenau, A. Patkowski, W. Steffen, and W. Thönnes, J. Non-Cryst. Solids **131-133**, 134 (1991).
[2] E. Leutheusser, Phys. Rev. A **29**, 2765 (1984); U. Bengtzelius, W. Götze, and A. Sjölander, J. Phys. C **17**, 5915 (1984); W. Götze, Phys. Scr. **34**, 66 (1986).
[3] See, for example, G. Williams, J. Non-Cryst. Solids **131-133**, 1 (1991), and references therein.
[4] E. W. Fischer, G. P. Hellmann, H. W. Spiess, F. J. Hörth, U. Ecarius, and M. Wehrle, Makromol. Chem. Suppl. **12**, 189 (1985).
[5] G. Meier and G. Fytas, in *Optical Techniques to Characterize Polymer Systems*, edited by H. Bassler (Elsevier, Amsterdam, 1989).
[6] E. Rössler, Phys. Rev. Lett. **65**, 1595 (1990).
[7] G. Fytas, A. Rizos, G. Floudas, and T. P. Lodge, J. Chem. Phys. **93**, 5096 (1990).
[8] E. Rössler, Ber. Bunsenges. Phys. Chem. **94**, 392 (1990).
[9] G. P. Johari and M. Goldstein, J. Chem. Phys. **53**, 2372 (1970).
[10] G. Floudas, W. Steffen, L. Giebel, and G. Fytas, Colloid Polym. Sci. (submitted).
[11] D. Boese, B. Momper, G. Meier, F. Kremer, J.-U. Hagenah, and E. W. Fischer, Macromolecules **22**, 4416 (1989).
[12] G. Floudas, G. Fytas, and E. W. Fischer, Macromolecules **24**, 1955 (1991).
[13] G. Floudas, A. Patkowski, G. Fytas, and M. Ballauff, J. Phys. Chem. **94**, 3215 (1990).
[14] H. C. Andersen and R. Pecora, J. Chem. Phys. **54**, 2584 (1971).
[15] G. D. Patterson and G. R. Alms, Macromolecules **10**, 1237 (1977).
[16] B. Berne and R. Pecora, *Dynamic Light Scattering* (Wiley-Interscience, New York, 1976).
[17] M. Bée, *Quasielastic Neutron Scattering* (IOP, Bristol, 1988).
[18] E. Bartsch, F. Fujara, M. Kiebel, H. Sillescu, and W. Petry, Ber. Bunsenges. Phys. Chem. **93**, 1252 (1989).
[19] W. Petry, E. Bartsch, F. Fujara, M. Kiebel, H. Sillescu, and B. Farago, Z. Phys. B **83**, 175 (1991).
[20] L. Börjesson and W. S. Howells, J. Non-Cryst. Solids **131-133**, 53 (1991); L. Börjesson, M. Elmroth, and L. M. Torell, Chem. Phys. **149**, 209 (1990).
[21] T. Keyes and D. Kivelson, J. Chem. Phys. **56**, 1057 (1974).
[22] Viscosity data for DOP: (a) A. J. Barlow, J. Lamb, and A. J. Matheson, Proc. R. Soc. London, Ser. A **292**, 322 (1966) ($233 < T < 370$ K); (b) R. Colby, Ph.D. thesis, Northwestern University, 1985 ($247 < T < 321$ K); (c) G. Floudas, Ph.D. thesis, University of Crete, 1990 ($303 < T < 352$ K); (d) L. Giebel, Ph.D. thesis, University of Mainz, 1991 ($223 < T < 367$ K); (e) Ind. Eng. Chem. **39**, 484 (1947) ($255 < T < 372$ K).
[23] G. Floudas, G. Fytas, and I. Alig, Polymer **32**, 2307 (1991).
[24] T. G. Oh, E. W. Fischer, G. P. Hellmann, T. P. Russell, and C. H. Wang, Polymer **27**, 261 (1986).

[25] D. A. Pinnow, S. J. Candau, J. T. LaMacchia, and T. A. Litovitz, J. Acoust. Soc. Am. **43**, 131 (1967).
[26] E. W. Fischer, Ch. Becker, J.-U. Hagenah, and G. Meier, Prog. Colloid Polym. Sci. **80**, 198 (1989).
[27] K. S. Singwi and A. Sjölander, Phys. Rev. **119**, 863 (1960).
[28] J. Teixeira, M.-C. Bellissent-Funel, S. H. Chen, and A. J. Dianoux, Phys. Rev. A **31**, 1913 (1985).
[29] T. Kanaya, K. Kaji, and K. Inoue, Macromolecules **24**, 1826 (1991).
[30] G. Meier, B. Gerharz, D. Boese, and E. W. Fischer, J. Chem. Phys. **94**, 3050 (1991).
[31] B. Gabryś, J. S. Higgins, K. T. Ma, and J. E. Roots, Macromolecules **17**, 560 (1984).
[32] G. Floudas and J. S. Higgins, Polymer (in press).
[33] G. Meier, F. Fujara, and W. Petry, Macromolecules **22**, 4421 (1989).
[34] K. Inoue, T. Kanaya, S. Ikeda, K. Kaji, K. Shibata, M. Misawa, and Y. Kiyanagi, J. Chem. Phys. **95**, 5332 (1991), and references therein.
[35] G. Floudas, G. Fytas, and W. Brown, J. Chem. Phys. **96**, 2164 (1992).
[36] D. Kivelson and S. A. Kivelson, J. Chem. Phys. **90**, 4464 (1989).
[37] C. H. Wang, G. Fytas, and J. Zhang, J. Chem. Phys. **82**, 3405 (1985).
[38] W. Petry, M. Kiebel, and H. Sillescu, in *Dynamics of Disordered Materials*, edited by D. Richter, A. J. Dianoux, W. Petry, and J. Teixeira (Springer, Berlin, 1989).
[39] J. Colmenero, A. Alegria, J. M. Alberdi, and B. Frick, J. Non-Cryst. Solids **131-133**, 949 (1991).
[40] This has also been observed in a recent neutron spin-echo study of bulk polyisoprene: R. Zorn, D. Richter, B. Farago, B. Frick, F. Kremer, U. Kirst, and L. J. Fetters, Physica B (in press).
[41] Recent data on propylene glycol [A. R. Duggal and K. A. Nelson, J. Chem. Phys. **94**, 7677 (1991)] and simple alcohols [M. A. Floriano and C. A. Angell, J. Chem. Phys. **91**, 2537 (1989)] revealed that DR times can be slower than light-scattering and mechanical relaxation times, especially at high T. In this context, it would be interesting to perform impulsive stimulated light-scattering experiments on DOP.
[42] A different behavior for the translational and the rotational diffusion has also been reported: M. Lohfink and H. Sillescu, Proceedings Tohwa Univ. Int. Symp., Fukuoka, Japan; Am. Inst. Phys. Conf. Ser. (in press).